Deep-Sea Research I 59 (2012) 25–36

Contents lists available at SciVerse ScienceDirect

Deep-Sea Research I

journal homepage: www.elsevier.com/locate/dsri

Variability of the Kuroshio in the East China Sea derived from satellite altimetry data

Zhiqiang Liu, Jianping Gan *

Division of Environment & Department of Mathematics, Hong Kong University of Science and Technology, Kowloon, Hong Kong

ARTICLE INFO

Article history:
Received 15 April 2011
Received in revised form
26 October 2011
Accepted 28 October 2011
Available online 7 November 2011

Keywords:
Kuroshio
Western boundary current
Along- and across-stream transport

ABSTRACT

We investigate the spatial and temporal surface variability along the entire Kuroshio Current in the East China Sea (ECS) using 16-year (1993–2008) surface geostrophic currents derived from satellite altimetry data. Our analysis is based on stream coordinate and physically sensible definitions of the axis, width, along- and cross-stream transports. Mainly flowing along the 200 m isobath, the Kuroshio's width narrows from ~218 km in the winter towards ~207 km in the summer while the surface transport increases from a minimum of 6.8×10^4 m^2/s in the autumn to a maximum of 7.4×10^4 m^2/s in the summer. The width, surface transport, and the magnitude of the along-stream velocity of the Kuroshio are positively correlated along its track and have relatively large values in the central ECS. The shoreward intrusion that departs from the mainstream chiefly occurs near the southwest of Kyushu where an estimated transport of 1.8 Sv of the Kuroshio veers towards the Tsushima Strait throughout the year. The surface shoreward intrusion in other parts of the Kuroshio is generally weak and most of the transport that deviates shoreward from the core (around the 200 m isobath) of the Kuroshio recirculates within the stream. The net surface transport induced by Ekman process along the stream contributes to the surface shoreward intrusion, and the intrusion in the entire vertical water column is, nevertheless, controlled by the local geostrophic current. The spatial structure of the intrusion is mostly governed by the response of stream to shelf topography between the 200 m isobath and the shore-side boundary. The transport across the shore-side boundary of the Kuroshio is considerably different from the transport across the 200 m isobath, and the former better reflects the water exchange between the stream and the ECS shelf.

1. Introduction

The Kuroshio Current is a strong western boundary current in the western North Pacific Ocean. It originates from a bifurcation of the North Equatorial Current off the east coast of the Luzon Islands at about 15°N. After flowing northward past Luzon Strait, where it exchanges with the South China Sea (Gan et al., 2006), the Kuroshio Current enters the East China Sea (ECS) through East Taiwan Strait (ETS), and exits through the Tokara Strait south of Kyushu Island (Fig. 1). The Kuroshio transports warm, tropical water northward along the shelf slope of the East China Sea (ECS). The Kuroshio mainly flows along 200 m isobath (Nitani, 1972), but part of the Kuroshio escapes from the constraint of bottom topography and intrudes into the ECS shelves. The main stream of the Kuroshio Current also bifurcates near 30°N due to the divergence of the isobaths (Hsueh, 2000).

In previous studies, spatiotemporal variability along the Kuroshio has been discussed based mainly on the measurements from isolated locations and over a relatively short time. Sun and Su (1994) found that the axis of the Kuroshio shifts shoreward northeast of Taiwan during the colder half year and seaward in the warmer half year because of monsoon forcing. The axis was found to have little seasonal variability (Ichikawa and Beardsley, 2002) along the PN section (Fig. 1) in the central ECS. Volume transport across this section was found to have a maximum of ~25.4 Sv in summer, a minimum of ~16.2 Sv in autumn, and an annual mean of 21.2 Sv. The volume transport exhibits spatial variations along the path of the Kuroshio Current. Lee et al. (2001) reported that stronger Kuroshio Current appears in the ETS and during the summer (~24 Sv), and weaker during the winter (~20 Sv). However, because of the limited coverage of the field measurements, the characteristics of spatiotemporal variability along the entire Kuroshio, based on long-term records, have not been adequately investigated.

The Kuroshio Current's shoreward intrusion greatly influences circulation over the ECS shelf and mainly occurs northeast of Taiwan and southwest of Kyushu (Nitani, 1972; Lee and Matsuno, 2007).

* Corresponding author.
E-mail address: magan@ust.hk (J. Gan).

0967-0637/$ - see front matter © 2011 Elsevier Ltd. All rights reserved.
doi:10.1016/j.dsr.2011.10.008

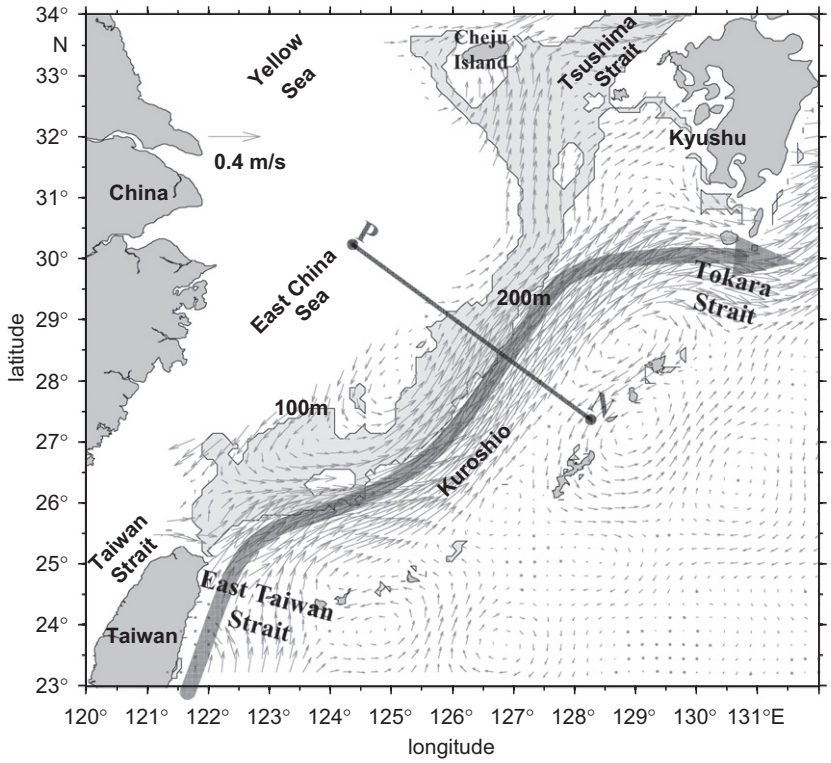

Fig. 1. Distribution of the 16-year (1993–2008), averaged, surface geostrophic velocity vectors in the ECS. The PN line (solid gray line) as well as the general features of the Kuroshio mainstream (bold gray arrow) are also illustrated.

The intrusion in these two locations is also the key mechanism that forms the Taiwan Warm Current (Teague et al., 2003; Isobe, 2008) and the Tsushima Warm Current (Sverdrup et al., 1942; Hsueh, 2000). However, due to the complexity of the flow field and the limited field measurements, the characteristics of the intrusion from both the region southwest of Kyushu and northeast of Taiwan over the broad ECS shelf remain unclear.

Unlike previous studies, this paper derives the characteristics of the spatiotemporal variability in the Kuroshio from the surface geostrophic currents along the entire Kuroshio (stream coordinate) rather than from an isolated portion (geographic coordinate). This study also uses a long-term record rather than a partial record in the ECS. We adopt a physically sensible concept to better characterize the axis, width, shore-side boundary, and transport of the Kuroshio. The general nature of the Kuroshio derived from the relatively broad spatiotemporal coverage of the surface currents in this study fills the gaps in understanding of the Kuroshio in the ECS.

2. Data and methods

2.1. Data

A 16-year (1993–2008) time series of merged absolute geostrophic velocity (AGV) data was used. The data is distributed by *Archiving, Validation, and Interpretation of Satellite Oceanographic Data* (AVISO), in France. The AGV was calculated from the Absolute Dynamic Topography (ADT) which is the sum of the Sea Level Anomaly (SLA) and the Mean Dynamic Topography (MDT). The MDT, acting as a mean surface elevation field in this study, is calculated by combining multiple data resources, including the Lagrangian drifting buoys, hydrological profiles, altimetric data and a geoid model (Rio and Hernandez, 2004), and thereby:

$$\mathrm{ADT} = \mathrm{SLA} + \mathrm{MDT}. \quad (1)$$

We selected 7-day averaged, "updated" and "gridded" data with some temporal and spatial smoothing (Ducet et al., 2000; Le Traon et al., 2001). These data were interpolated from well-validated, along-track data (e.g. Hwang and Kao, 2002; Zhu et al., 2004; Andres et al., 2008a). They were found to have a high correlation coefficient (>0.8) with the sub-tidal, long term, observed data east of Taiwan (Hwang, 1996). The "updated" data merges data from four satellites (TOPEX/Poseidon and Jason-1, ERS1/2, Envisat, Geosat) and the word, "gridded", denotes a weekly average on a 1/3° Mercator grid. These data were also validated, for example, by Pascual et al. (2007).

2.2. Methods

Traditionally, the main stream of the Kuroshio Current was thought to be located between the 100 m and 2000 m isobaths with a velocity larger than that of neighboring currents. We treated the Kuroshio Current as a jet with velocity decreasing from its maximum velocity at its core/axis (Fig. 2). An axis for the Kuroshio was obtained from the 1/10° gridded data of the flow field that were interpolated from the 1/3° original data. The width of the Kuroshio at any given location was defined to be the length between P and Q (Fig. 2) of a section normal to the jet axis with a cut-off velocity (v_o) in along-stream direction (normal to PQ). The v_o was selected as 0.1 m/s in this study, after evaluations from sensitivity experiments with different values of v_o, and from the flow field (Section 3). The along-stream surface transport (AT) was then derived by

$$\mathrm{AT} = \int_P^Q V^{norm} ds, \quad (2)$$

where V^{norm} is the velocity normal to the section (or parallel to the axis) of the Kuroshio, and ds is the distance between two neighboring points across the width of the Kuroshio (Fig. 2). We assumed that the Kuroshio decelerated linearly with depth at any

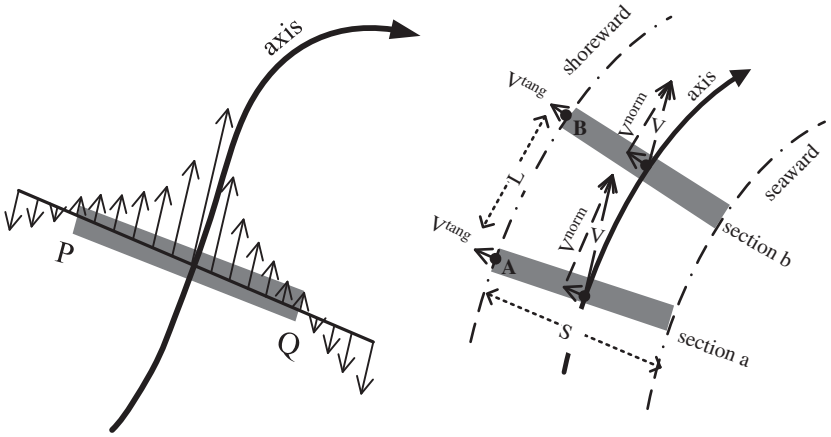

Fig. 2. Schematic definitions of the width (shaded length between P and Q), axis, the shore-side and sea-side boundaries, and the shoreward (V^{tang}) and along-stream (V^{norm}) velocities along Kuroshio.

given section and that its velocity profile across the vertical transect had a parabolic shape when we estimated the total transport. This approximation is supported by the field measurement of Johns et al. (2001) in the ETS and by the geostrophic velocity profile derived from long-term (1989–1997) hydrographic observation along the PN line (Oka and Kawabe, 2003; Andres et al., 2008b).

Unlike previous studies that commonly used a shoreward velocity crossing the 200 m isobath to represent the shoreward transport, we defined the shoreward velocity of the Kuroshio (V^{tang}) as the velocity normal to its shore-side boundary at the edge of the jet-shaped Kuroshio (Fig. 2), and the same definition is applied to the sea-side boundary. Thus, the total surface shoreward transport integrated along the shore-side boundary of Kuroshio is

$$CT = \int_{along\ axis} V^{\mathrm{tang}} dl. \tag{3}$$

Positive *CT* represents the *true* transport, or surface transport, that departs from the Kuroshio mainstream and intrudes farther shoreward. It is a better reflection of the shoreward intrusion of the Kuroshio compared to the one that crosses the 200 m isobath because it excludes the transport that is recirculated back to the Kuroshio and that flows northeastward after crossing the 200 m isobath.

3. Results

Along the stream-coordinate, we calculate the terms including position of axis and shore-side boundary as well as surface transport in both along-stream and cross-stream directions every 7 day. The mean value, seasonal and inter-annual variations as well as their variances are presented and discussed.

3.1. Mean Kuroshio pattern

The 16-year mean surface velocity field (Fig. 1) shows that the Kuroshio enters the ECS through the ETS, and the main stream flows northeastward along the 200 m isobath before deviating eastward from the 200 m isobath at about 29°N (red solid line in Fig. 3). The Kuroshio subsequently forms an eastward main stream towards Tokara Strait and a northward stream towards Tsushima Strait (Fig. 1). The standard deviation (STD) of the core position (red dashed lines in Fig. 3) indicates that the Kuroshio's axis has an overall variation of less than 50 km along its path. The shore-side boundary, where the V^{norm} of the Kuroshio decreases to 0.1 m/s (green solid curve in Fig. 3), is mainly located on the ECS shelf between the 100 m and the 200 m isobath and is directed generally along the Kuroshio's axis. Spatially, deviation of the shore-side boundary from its mean position during the 16-years is less than 65 km (green dashed lines in Fig. 3). The boundary matches the current field well in Fig. 1 and the spatial correlation of the shore-side boundary with the axis of the Kuroshio itself suggest that the boundary is mostly associated with the main stream. The boundary derived from $v_o = 0.4$ m/s (blue curve in Fig. 3) tends to be too close to the Kuroshio core while the boundary derived from $v_o < 0.1$ m/s is not well defined due to interaction with other shelf currents at the far edge of Kuroshio. The shore-side boundary of the Kuroshio southwest of Kyushu shows a relatively large spatial variation of about 75 km between 126.2°E and 128°E, which is reflected in the corresponding STD values (green dashed lines in Fig. 3).

The shoreward intruding Kuroshio in the region northeast of Taiwan at 122°E 25.6°N has been reported in many previous studies (e.g. Lee and Matsuno, 2007). However, the surface flow field shows that, after turning westward and crossing the 200 m isobath off northeastern Taiwan, part of the shoreward intrusion swings back to the main stream between the 100 m and 200 m isobaths and then it flows northeastward. The apparent shoreward intrusion along the Kuroshio occurs in the waters southwest of Kyushu, where a northward current leaves the main stream of the Kuroshio, crosses the shore-side boundary, and then flows towards Tsushima Strait.

The 16-year mean width, surface transport and velocity along the Kuroshio's axis, and the shoreward velocity (V^{tang}) along the shore-side boundary are shown in Fig. 4. The average width along the Kuroshio is ~210 km, which is close to the 225 km estimated based on the Munk's (1950) theorem of western boundary currents when lateral eddy friction is $A_H = 5 \times 10^3$ m^2/s, and the STD is less than 50 km along the Kuroshio mainstream. Accordingly, the sea-side boundary varies little from its core position as indicated in Fig. 3. (solid and dashed orange lines). The 16-year averaged surface transport is about 7.17×10^4 m^2/s, with the STD about 0.7×10^4 m^2/s along the Kuroshio mainstream. With the undercurrent flowing southwestward opposite to the direction of Kuroshio in the bottom layer of the Okinawa Trough, the Kuroshio may not always reach the bottom. If we use the assumptions that the Kuroshio linearly decreases with depth and that there is a parabolic velocity profile (see Section 2) with a maximum influence depth of 800 m (Oka and Kawabe, 2003; Andres et al., 2008b), the estimate of the mean transport of the Kuroshio would

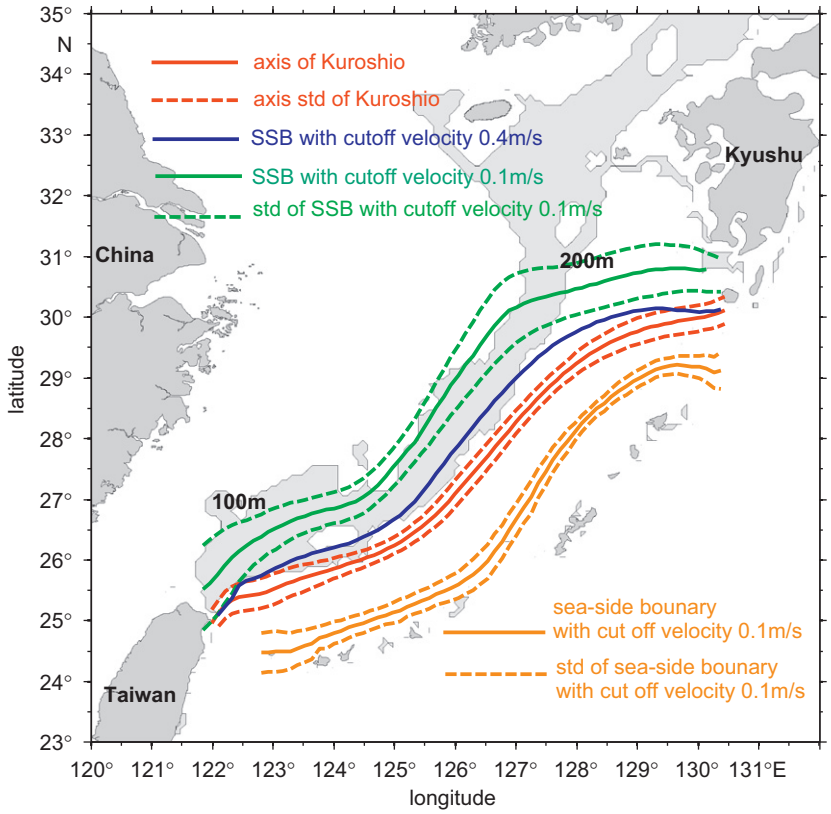

Fig. 3. Distribution of the 16-year (1993–2008) averaged location of the Kuroshio's axis (red solid line) and its standard deviation (STD, red dashed lines), and shore-side boundary of the Kuroshio (green solid line) and its STD (green dashed lines), as well as the shore-side boundary of the sensitivity experiment using a 0.4 m/s cut-off velocity (blue solid line). Location of the sea-side boundary (orange solid line) and its STD (orange dashed lines) are also demonstrated. Water between the 100 m and the 200 m isobaths are shaded, and "SSB" represents the shore-side boundary. (For interpretation of the references to color in this figure legend, the reader is referred to the web version of this article.)

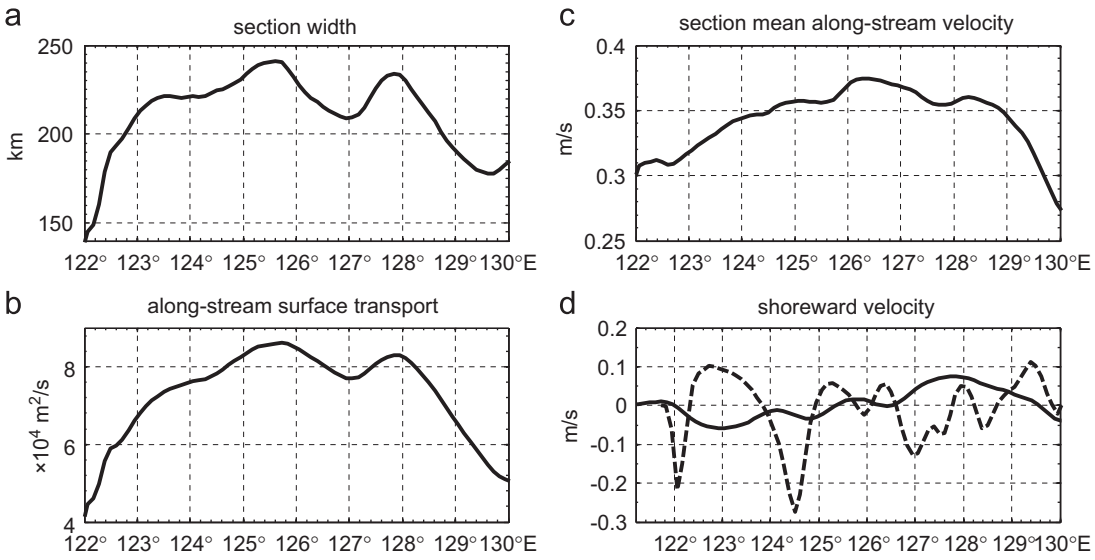

Fig. 4. Distribution of (a) section width; (b) along-stream surface transport; (c) section mean along-stream velocity; and (d) velocity across the shore-side boundary as a function of longitude. The velocity across the 200 m isobath is also displayed by the dashed line in (d). Positive values are directed northward in (b) and (c), and shoreward in (d).

be ~20.4 Sv. This is comparable to the 21.2 Sv suggested by previous studies (e.g. Ichikawa and Beardsley, 2002).

The section width and along-stream surface transport (Fig. 4a and b) vary coherently with a correlation coefficient (CC) of about 0.95 and the significant level (SL) is 5%. The width and along-stream surface transport increase from 122°E and reach relatively large values at 125.5°E and 128°E. One possible explanation for the increase of the Kuroshio width from 122°E is likely due to diverging of the isobaths where the topographic gradients decreases. The Kuroshio mainstream expands shoreward on the surface layer and

widens the stream along its track. The strength of the surface Kuroshio remains relatively uniform in the central part of the ECS between 125°E and 128°E, but it becomes weaker south and north of this region. The section mean velocity (Fig. 4c) in the along-stream direction exhibits similar spatial patterns as the width (CC=0.71, SL=5%) and the along-stream surface transport (CC=0.89, SL=5%). The surface Kuroshio accelerates from 122°E to 126.5°E, and then decelerates from 126.5°E to about 127.8°E. The spatial characteristics of the Kuroshio Current may be largely controlled by the local topography.

The shoreward velocity across the shore-side boundary (Fig. 4d solid line) is very small at 122°E northeast of Taiwan. This is followed by a negative, or seaward, velocity farther north in the portion of the stream from 122°E to 125°E. The shoreward intrusion southwest of Kyushu, between 126.4°E and 129.4°E, has a maximum value at 127.6°E. Based on field measurement, Lie et al. (1998) showed that the Kuroshio intrusion southwest Kyushu occurred from the surface to the bottom (100 m) in the water column with relatively weak stratification. Accordingly, the estimation of the shoreward transport southwest of Kyushu would be about 1.8 Sv. The process that increases the shoreward surface velocity of the Kuroshio near 127.8°E is likely due to the forcing from the local shoreward convex isobaths (Gan et al., 2009).

For comparison, the shoreward velocity across the 200 m isobath is also shown in Fig. 4d (dashed line). There is a shoreward branch from the main stream between 122.3°E and 123.8°E, northeast of Taiwan. This branch, however, is shifted seaward downstream because of the strong recirculation between 123.8°E and 124.8°E. Qiu and Imasato (1990) also found the similar shoreward intrusion and the subsequent seaward shift of the Kuroshio. There is no evidence that the surface Kuroshio, moving westward across the 200 m isobath, between 122.3°E and 123.8°E, reaches the shore-side boundary. In contrast to the strong shoreward velocity across the shore-side boundary, between 126.5°E and 129.4°E, the shoreward intrusive currents southwest of Kyushu are absent in the velocity across the 200 m isobath at the same location. Because the shoreward intrusion of the Kuroshio southwest of Kyushu has been widely reported (e.g. Hsueh et al., 1996; Lie and Cho, 2002), it is conceivable that the transport across the 200 m isobath may not properly represent the Kuroshio's shoreward intrusion.

Different from the *AGV* data utilized in this study (Section 2.1), Ma et al. (2009) retrieved the surface velocity fields in the ECS by using Argos drifter buoys for *MTD* and TOPEX/POSEIDON altimeter data for *SLA* to study the variation of Kuroshio along the sections between Luzon Strait and Tokara Strait. To further validate the surface velocity fields obtained from the AVISO absolute geostrophic current, we also conducted the above calculations by using the surface velocity field of Ma et al. (2009). The spatially-averaged Kuroshio width (~200 km), surface transport (~7.8×10^4 m^2/s), and along-stream velocity (~0.39 m/s) from the database of Ma et al. (2009) are reasonably close to the results shown in Fig. 4.

3.2. Seasonal variability of Kuroshio

The seasonal average of the Kuroshio's axis and its shore-side boundary (Fig. 5) display very similar patterns to those of the mean fields. The seasonal change of the axis is small. It has a relatively large variation northeast of Taiwan where the axis shifts mostly shoreward in the winter and mostly seaward in the summer from its axis/core around the 200 m isobath. The location of the shore-side boundary generally has the same seasonal pattern as the axis. Relatively larger spatial variation of ~50 km with opposite seasonal tendency occurred in the northeast of Taiwan and southwest of Kyushu (Fig. 5 dashed lines), where

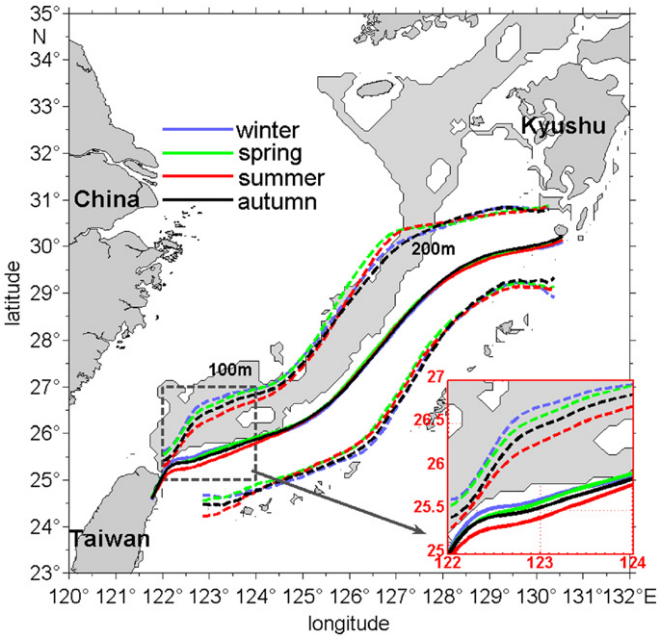

Fig. 5. Seasonal mean of the Kuroshio's axis (solid curves) and its shore-side boundary (dashed curves between 100 m and 200 m isobaths). The seasonal mean of sea-side boundary (dashed curves on the offshore areas) are also plotted.

the shore-side boundary moved seaward/shoreward in the summer and shoreward/seaward in the winter.

Seasonal mean of the velocity distribution (not shown) is very similar to that of the mean field (Fig. 3). Northeast of Taiwan, there is a weak surface current across the shore-side boundary and flowing towards the coast near 122°E 25.6°N, especially during the winter and spring. At the same time, the northward bifurcation of the Kuroshio Current southwest of Kyushu persists in all seasons. An anti-cyclonic eddy can be identified to the south of Kyushu, similar to the finding of Hsueh et al. (1996).

Seasonal variations of the magnitudes of the section width, surface along-stream transport, section-averaged along-stream velocity, and shoreward velocity at the shore-side boundary are generally weak along the ECS shelf (Fig. 6). Along-stream-average section width has a maximum value of ~218 km (Fig. 6a) in the winter and a minimum of ~207 km in the summer. Northeast of Taiwan, at 124.8°E, the Kuroshio widens ~40 km from summer to winter, while the opposite condition occurs southwest of Kyushu at 128°E. The width varies less than 25 km elsewhere along the stream and among the seasons. Larger mean surface along-stream transport occurs in the summer (~7.4×10^4 m^2/s) and the spring, and smaller values appear in the winter and the autumn (~6.8×10^4 m^2/s Fig. 7b). The section mean along-stream velocity (Fig. 6c) has a relatively large velocity in spring and summer. The variations of the section width, surface along-stream transport, and section mean Kuroshio velocity indicates that the stronger Kuroshio occurs in summer with a larger transport, but with a narrower main stream.

Northeast of Taiwan, around 122°E, the shoreward velocity across the shore-side boundary has a very small value in winter when the Kuroshio is relatively weak (Fig. 6d, colored solid lines). It becomes almost zero and directs seaward during the other three seasons. East of 122°E, the seaward currents occur at the shore-side boundary near 123°E. However, the velocity across the 200 m isobath (Fig. 6d, colored dashed lines) has a clear seasonal variation with much larger values (>0.1 m/s) in spring and summer. This is different from the velocity across the shore-side boundary of the Kuroshio, which generally flows shoreward between

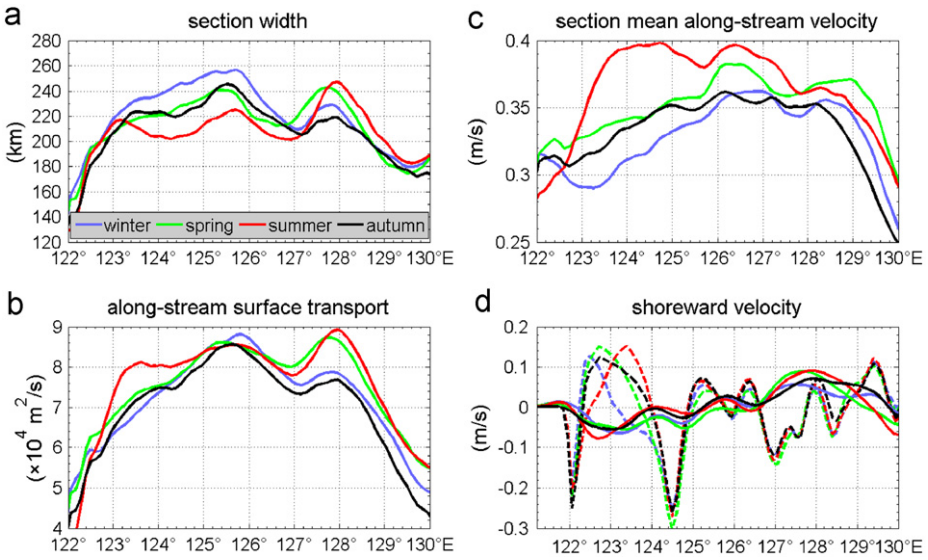

Fig. 6. Same as Fig. 4, but for the winter, spring, summer, and autumn. (For interpretation of the references to color in this figure legend, the reader is referred to the web version of this article.)

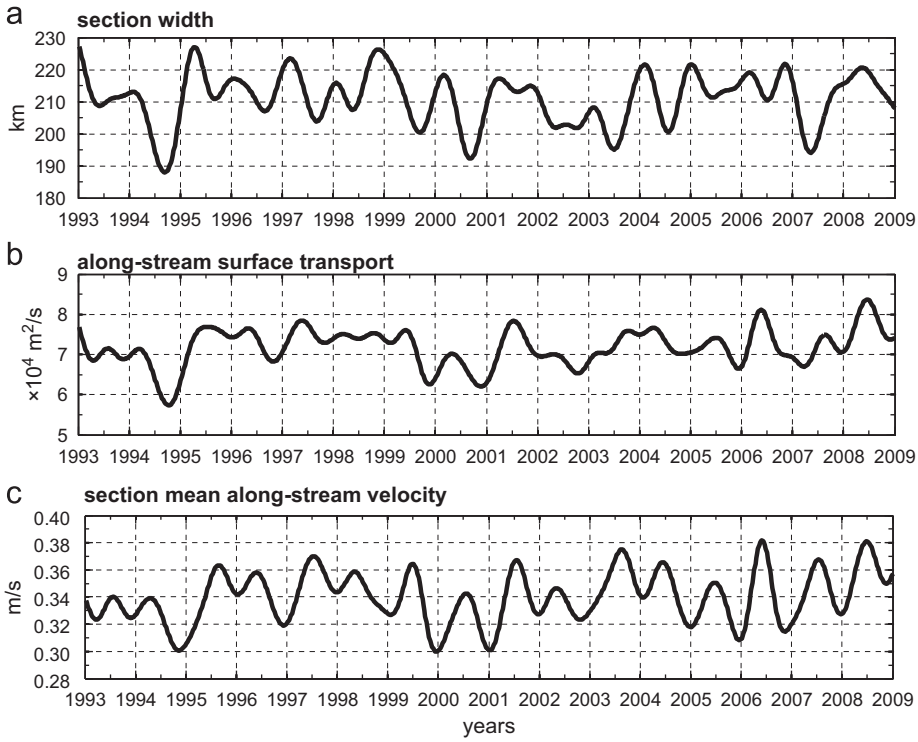

Fig. 7. Time-series of 1/2 year filtered mean (a) section width, (b) along-stream surface transport, and (c) section averaged along-stream velocity from 122°E to 130°E. The positive values in (b) and (c) are mainly directed northeastward.

122.2°E and 124°E and seaward between 124°E and 125°E. By comparing the transports that cross the 200 m isobath to those that cross the shore-side boundary of the Kuroshio, we find that most of the westward movement across the 200 m isobath, west of 124°E, recirculate back to or flow northward with the mainstream and cannot reach the shore-side boundary in all seasons.

Southwest of Kyushu, the seasonal variation of the shoreward intrusion is relatively weak. The shoreward velocity across the shore-side boundary peaks near 127.8°E during all seasons. A relatively large shoreward velocity appears in summer and spring, while a smaller one occurs in winter and autumn. Oppositely, the width of the intrusive current is ~313 km extending from 126.8°E to 129.8°E during the winter and autumn and ~269 km from 126.8°E to 129.4°E during the summer and spring. However, the shoreward velocity across the 200 m isobath is mainly directed seaward during all seasons in this region. Thus, it is conceivable that the shore-side boundary, rather than the 200 m isobath, is a more accurate reference to define the intrusion of the Kuroshio onto the ECS shelf.

3.3. *Inter-annual variability of Kuroshio*

The Kuroshio Current also varies inter-annually. Fig. 7 shows the time series of section width, surface along-stream transport, and section-averages of along-stream velocity between 122°E and 130°E from 1993 to 2008. Besides the embedded seasonal variations

(Section 3.2), there were strong inter-annual characteristics in these three variables. A relatively weak current occurred in 1994, 2000, and 2002, while a strong one occurred in 1995, 1997, 2001, 2006, and 2008. A strong correlation exists between the surface along-stream transport and the section mean along-stream velocity (CC=0.77, SL=5%). The correlation between the section width and the corresponding surface along-stream transport is about CC=0.61 (SL=5%) with a one-month lag in the transport, while the velocity and the transport is generally in phase. Spatially, the variation of section width, surface along-stream transport, and section mean along-stream velocity during the 16 years (Fig. 8) show the same pattern as the variation in Figs. 4 and 6. In most years, relatively large values of width and transport appeared near the two peaks centered on 125.5°E and 128°E while a smaller spatial varying and larger velocity existed between them. The widening of the Kuroshio thus is a key factor controlling its surface transport.

Shoreward velocities across the shore-side boundary have inter-annual variation (Fig. 9a) and are not temporally correlated with

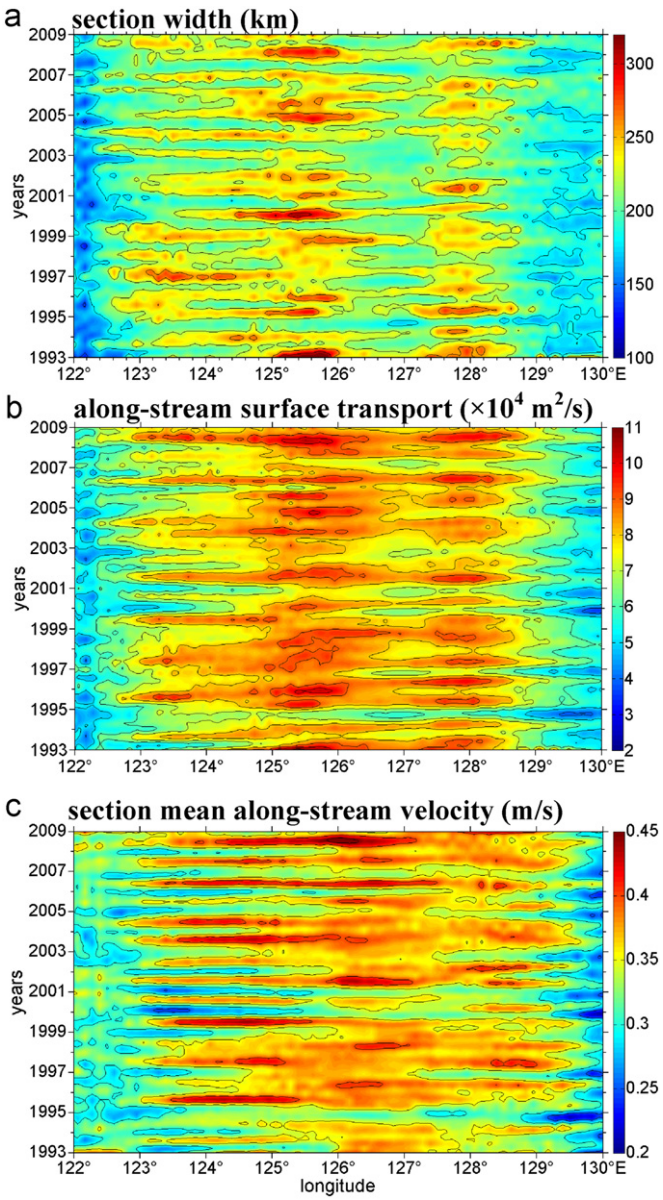

Fig. 8. 1/2 year filtered time series of the 16-year (1993–2008) Kuroshio (a) section width, (b) along-stream surface transport, and (c) section-mean along-stream velocity. The positive values are directed northward in (b) and (c).

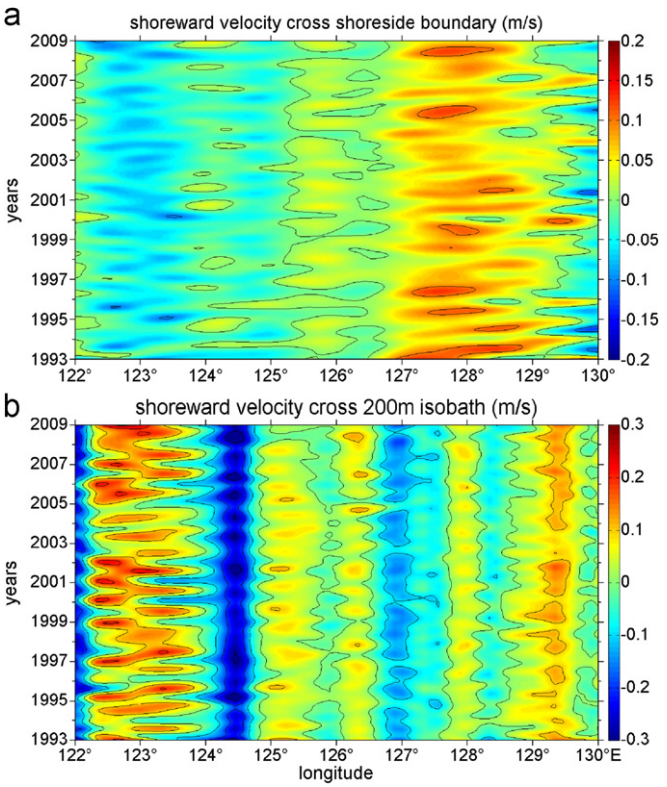

Fig. 9. 1/2 year filtered time series of the 16-year (1993–2008) Kuroshio (a) shoreward velocity across the shore-side boundary (b) across the 200 m isobaths. The positive values refer to the shoreward transport.

above variables. The intrusions northeast of Taiwan around 122°E and 122.4°E were slightly strong in the winter during most of the 16 years, especially during 1993, 2000, and 2008. The intrusion was absent in 1999 and 2002. This variation confirms that the surface intrusion northeast of Taiwan was not a persistent event and that it has strong inter-annual variability. The main surface on-shore intrusion of the Kuroshio water occurred southwest of Kyushu between 126.6°E and 129°E throughout the 16 years. The maximum intrusive velocity in this region was generally >0.1 m/s, except for 1997, 2002, 2003, 2006, and 2007. There was no large exchange of water between the Kuroshio and the ECS shelf between the northeast of Taiwan and the southwest of Kyushu.

The spatial and temporal variability of the shoreward velocity across the 200 m isobath (Fig. 9b) was largely different from that of the velocity across the shore-side boundary. Although there was considerable on-shore intrusion of the Kuroshio northeast of Taiwan, most of the intrusive current recirculated downstream between 123.8°E and 124.8°E or flowed northward with the Kuroshio shoreside of the 200 m isobath. The absence of an obvious shoreward intrusion across the 200 m isobath southwest of Kyushu, from 126.6°E to 129°E, during the 16 years, further suggests that the transport across the 200 m isobath mainly reflects the flow conditions around the core of the Kuroshio and cannot well represent the water exchange between the ECS and the Kuroshio Current.

4. Discussion

4.1. Effect of wind forcing

Although wind forcing contributes to the formation of a geostrophic current by setting up the pressure field, the surface Ekman drift (Ekman, 1905) has been neglected in the previous

analyses. Its effect on the Kuroshio is examined here. The surface Ekman current can be calculated by

$$\begin{cases} u(0) = V_0 \cos(\pi/4) \\ v(0) = V_0 \sin(\pi/4), \end{cases} \quad (4)$$

where the $u(0)$ and $v(0)$ refer to the eastward and northward surface Ekman velocity, respectively, and V_0 is the Ekman velocity (Ralph and Niiler, 1999):

$$V_0 = \frac{0.0068}{\sqrt{\sin|\varphi|}} U_{10}, \quad (5)$$

U_{10} is the wind speed above 10 m of the ocean surface and φ is the latitude. The wind speed is obtained from the monthly updated Scatterometer Climatology of Ocean Winds (SCOW) that was derived from QuikSCAT scatterometer data from September 1999 to October 2009 (Risien and Chelton, 2008). The total Ekman transport is given by

$$V_t = \frac{\tau}{\rho_0 f}, \quad (6)$$

where V_t is the total Ekman transport (or Ekman drift), τ is the wind stress, f is the Coriolis parameter, and ρ_0 is surface seawater density.

The 16-year average of monthly surface Ekman velocity and total Ekman transport along the stream, between 122°E and 130°E, are presented in Fig. 10. The contribution of surface Ekman currents to the surface along-stream transport and to the total shoreward transport is governed by the seasonal signal in the East Asia monsoon. In the along-stream direction (Fig. 10a and c), the southeasterly summer monsoon enhances the Kuroshio surface velocity and transport from May to August, while the stronger northeasterly monsoon suppresses them in other seasons. Because of asymmetric intensity in the seasonal wind forcing, the strength of the Kuroshio is weakened by the Ekman forcing on an annual time scale. Nevertheless, the surface transport contributed by Ekman currents is less than 7.6% of the 16-year averaged surface along-stream geostrophic transport of 7.17×10^4 m^2/s (Fig. 4a). Furthermore, the total Ekman transport within the Ekman layer is less than 0.7% of the total geostrophic volume transport of 20.4 Sv. The Ekman-induced shoreward transport across the shore-side boundary (Fig. 10b and d) had an opposite seasonal effect in summer and winter. It suppressed the shoreward intrusion of the surface Kuroshio in summer, but enhanced it during other seasons. The 16-year along-stream mean surface Ekman transport across the shore-side boundary was shoreward with a magnitude $\sim 1.02 \times 10^4$ m^2/s (Fig. 10b). With the seaward magnitude $\sim -0.21 \times 10^4$ m^2/s obtained in the corresponding geostrophic current, the total surface intrusion induced by both processes was shoreward with magnitude $\sim 0.81 \times 10^4$ m^2/s. It should be noted that although net surface shoreward intrusion integrated along the entire stream is mainly contributed by the Ekman transport, the shoreward transport in the entire vertical water column along the stream is largely controlled by the geostrophic current. The offsetting between the shoreward transport north of 127.75°E and the seaward transport south of 127.75°E makes the net transport from surface geostrophic transport relatively small (see Section 4.2).

4.2. Shoreward intrusion of the Kuroshio

There were few studies of the shoreward intrusion based on long-term data along the entire stream. The volume of water exchange between the Kuroshio Current and the ECS has often been estimated by the mass balance over the ECS among the transports across the Taiwan Strait in the south, Tsushima Strait in the north, and the Kuroshio intrusion in the east. Isobe (2008) suggested that the net supplement of water from the Kuroshio should be 1.4 Sv to compensate for the imbalance of the transport between the Taiwan Strait (1.2 Sv) and Tsushima Strait (2.6 Sv) over the shelf. In most of the previous studies, the 200 m isobath was frequently defined as the major interface for water exchange between the Kuroshio and the ECS. This is not accurate because the transport crossing the 200 m isobath flows mainly northward with the Kuroshio Current without entering the ECS at all, as we have shown in the previous discussion.

Fig. 11 shows the relationship between the shore-side boundary and the 200 m isobath as well as their corresponding transports. The 16-year, mean shore-side boundary intersects the 200 m isobath at about (30.4°N, 127.75°E) southwest of Kyushu (point ***M*** in Fig. 11). The intersection point divides the area into southern (between **b** and **e**) and northern (between **c** and **f**) subareas as marked in Fig. 11. The spatial distribution of the 16-year, mean velocities normal to the 200 m isobath is considerably

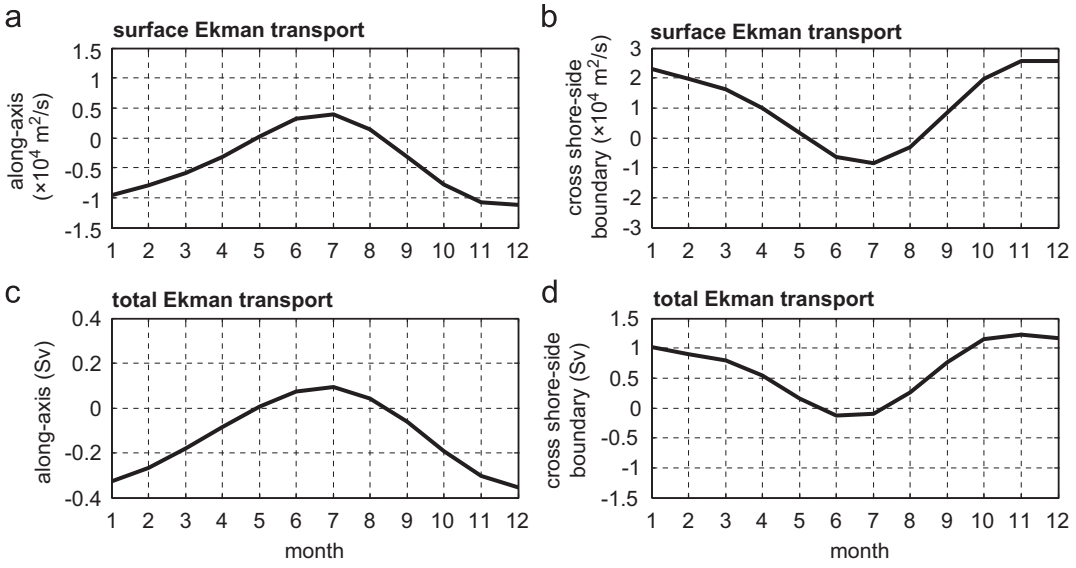

Fig. 10. Time series of (a) mean along-axis and (b) shoreward surface transport across the shore-side boundary, integrated from 122°E to 130°E from the surface Ekman velocity; (c) along-axis; and (d) across the shore-side boundary volume transport in the Ekman layer. Positive and negative values refer to the shoreward and seaward transports, respectively.

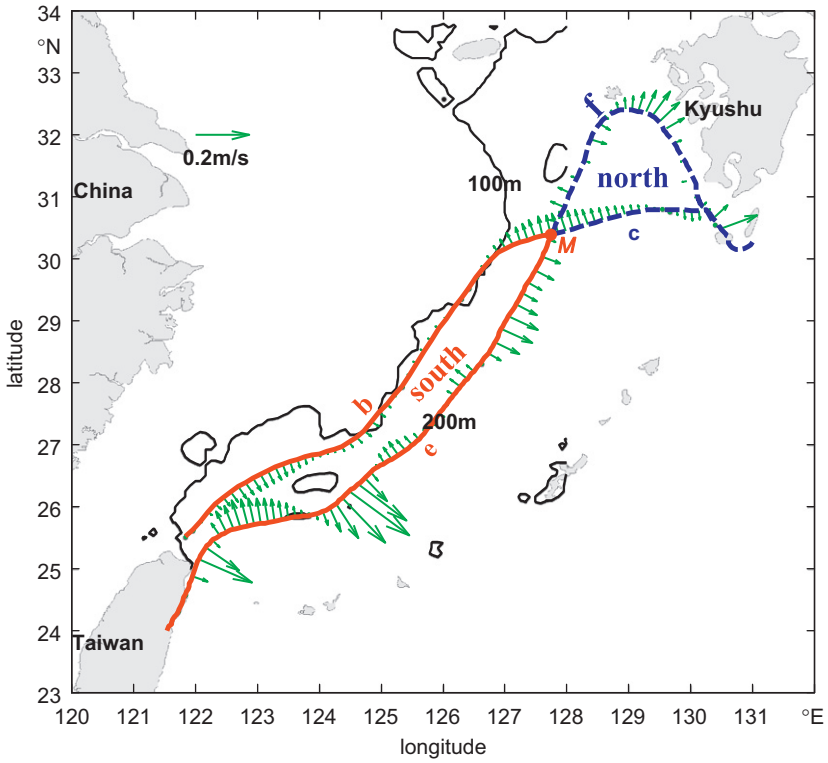

Fig. 11. Intersection point (***M***) of the 200 m isobaths (**e**+**f**) and 16-year (1993–2008) averaged shore-side boundary (**b**+**c**), as well as the north (blue dashed areas) and south (red solid areas) sub-areas. The 16-year averaged shoreward velocity vectors are also plotted (green vectors). (For interpretation of the references to color in this figure legend, the reader is referred to the web version of this article.)

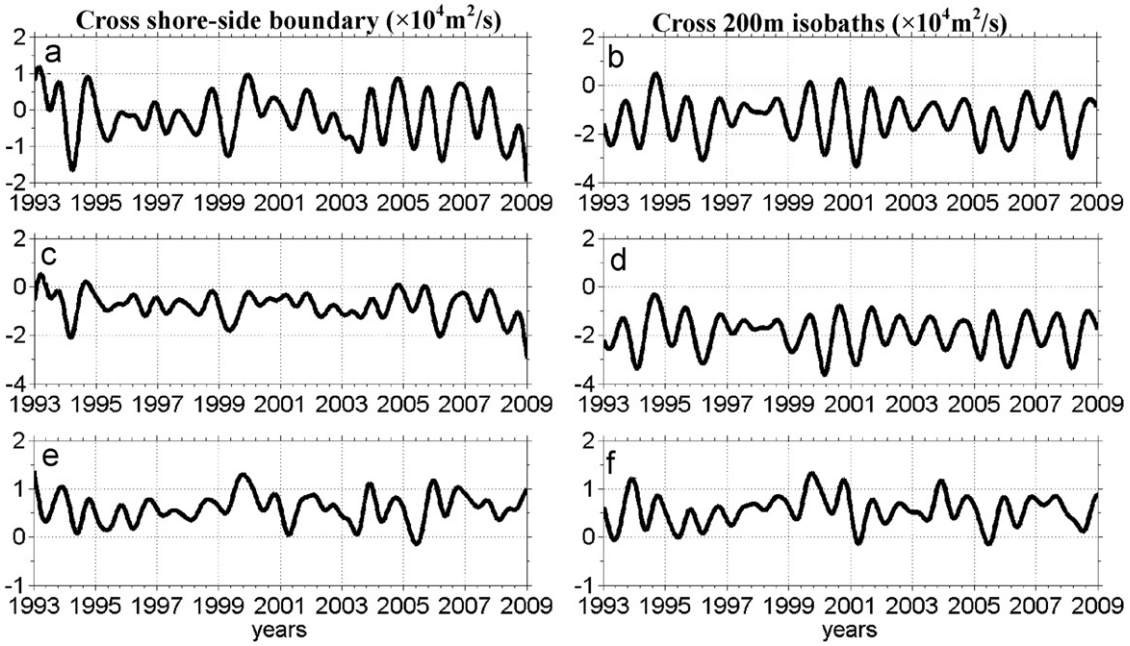

Fig. 12. Time-series of 1/2 year filtered total surface shoreward transport integrated from 122°E to 130°E for (a) across the shore-side boundary, (b) across the 200 m isobaths, (c) across shore-side boundary of the south sub-area, (d) across the 200 m isobaths of the south sub-area, (e) across the shore-side boundary of the north sub-area, and (f) across the 200 m isobaths of the north sub-area. Positive values refer to the shoreward transport.

different from that of the velocities normal to the shore-side boundary (Figs. 4d, 6d, and 9). Apparently, south of the southern sub-area, although the Kuroshio intrudes across the 200 m isobath, there is not a strong shoreward velocity on the shore-side boundary. North of the southern sub-area, although no shoreward current can be identified on the 200 m isobath, there is a shoreward velocity crossing the shore-side boundary between the 100 m and 200 m isobath.

The integrated surface shoreward transport along the entire shore-side boundary (**b**+**c**) and along the 200 m isobath (**e**+**f**) between 122°E and 130°E are shown in Fig. 12a and b. The figures show a very small correlation (CC=0.25, SL=5%) between the two

surface transports and that the 16-year averaged seaward surface transport was smaller across the shore-side boundary (-0.21×10^4 m^2/s) than the one across the 200 m isobath (-1.37×10^4 m^2/s). Both show a net surface seaward transport. The southern sub-area (Fig. 12c and d) shows almost the same pattern with CC=0.26, SL=5%. It has a smaller seaward surface transport on the shore-side boundary (-0.79×10^4 m^2/s) than across the 200 m isobath (-1.91×10^4 m^2/s). The northern sub-area (Fig. 12e and f) is totally different from the southern one with much larger correlations (CC=0.81, SL=5%) and very close intrusion strengths along the shore-side boundary (0.59×10^4 m^2/s) and along the 200 m isobath (0.55×10^4 m^2/s).

The calculation for the southern sub-area indicates that the larger surface shoreward intrusion crossing the shore-side boundary is not mainly determined by the surface Kuroshio transport crossing the 200 m isobath. Instead, the major process is probably associated with sub-surface upwelling of the Kuroshio along the ECS slope south of 30.4°N. The relatively larger contributions from the sub-surface and bottom layer have been confirmed by many field and modeling estimates (e.g. Ichikawa and Beardsley, 2002; Guo et al., 2006; Lee and Matsuno, 2007). We also found that the velocities normal to the shore-side boundary were spatially correlated (CC=0.61, SL=5%) with the intensity of the Kuroshio between the shore-side boundary and the axis. In contrast, it had little spatial correlation with the surface transport across the 200 m isobath. The result suggests that the intrusion intensifies where the Kuroshio is strong. The transport across the shore-side boundary can be generated by, for example, the pressure gradient along the boundary setup by the interaction between the Kuroshio Current and local shelf topography.

The spatial contribution of wind to the shoreward intrusion of the Kuroshio across the shore-side boundary is presented in Fig. 13. The contribution from the wind to the total shoreward surface velocity varied along the boundary. It had relatively large values in the regions between 124°E and 125°E as well as in the south and north of 128°E. Although the along-stream-average surface shoreward intrusion is mainly contributed by the Ekman current, as shown in Section 4.1, the contribution from the wind in isolated locations along the stream was much smaller compared to that from the geostrophic velocity. The geostrophic velocity mainly determined the spatial characteristics of the shoreward intrusion in the entire water column and across the shore-side boundary. Nevertheless, when considering the volume transport integrated over the Ekman layer, Ekman drift of about 0.54 Sv (Fig. 10d) accounts for about 38% of the 1.4 Sv total shoreward transport in the water column (Isobe, 2008).

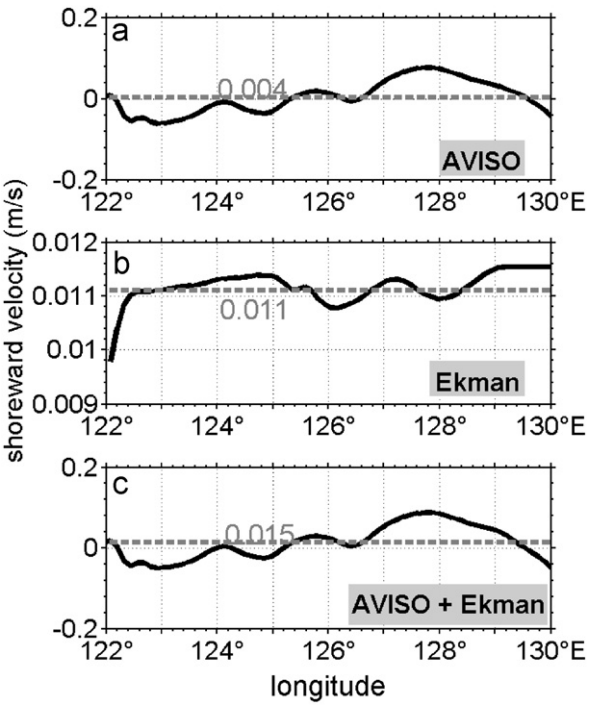

Fig. 13. Spatial distribution of mean surface velocities across the shore-side boundary obtained from (a) AVISO (same as Fig. 4d dashed line), (b) surface Ekman velocity, and (c) total velocity.

A composite of the 19 years (1991–2009) of seasonal surface drifter tracks along the shelf slope of the ECS (Fig. 14) further supports the findings presented in this study. Most of the drifters released east of Taiwan and along the ECS shelf slope flowed along the Kuroshio axis throughout the year. The shoreward movement of the drifters across the shore-side boundary mainly occurred northeast of Taiwan and southwest of Kyushu. Northeast of Taiwan, most of the drifters that crossed the 200 m isobath recirculated back to the main stream without entering the central ECS. Southwest of Kyushu, there were more drifters across the shore-side boundary that moved towards Tsushima Strait, although most of drifters continued to travel along the 200 m isobath.

5. Summary and conclusion

A 16-year (1993–2008) surface geostrophic velocity, derived from satellite altimetry data, was utilized to investigate the spatial and temporal variability of the near-surface Kuroshio Current in the ECS. By using physically sensible definitions of the axis, shore-side boundary, section width, along- and cross-stream transport/velocity and based on a stream instead of geographic coordinate, we derived the long-term mean intensities of Kuroshio as well as its seasonal and inter-annual variability along the mainstream. The general nature of the Kuroshio derived from the relatively broad spatiotemporal coverage of the surface currents in this study fills the gap of understanding of the processes along the Kuroshio over the ECS.

The Kuroshio exhibits strong spatiotemporal variability along its stream. It flows northward along the 200 m isobath until it bifurcates towards Tokara Strait and Tsushima Strait near 29°N. Averaged along the entire stream, the widest (~218 km) and the narrowest (~207 km) Kuroshio appear in winter and summer, respectively, with the annual mean width ~210 km. The 16-year averaged, along-stream mean transport is ~20.4 Sv. The width, surface transport, and the magnitude of the along-stream velocity are positively correlated along the Kuroshio's stream. They have relatively large values in the central ECS. The axis of the Kuroshio has little spatiotemporal variability over the ECS shelf except northeast of Taiwan and southwest of Kyushu. Northeast of Taiwan, the Kuroshio moves closer to the 200 m isobath, mostly in winter, and away from it in summer. Southwest of Kyushu, the Kuroshio turns eastward and deviates from the 200 m isobath.

Considering that the transport deviates from the core of the jet and moves downstream within the stream or recirculate back to the core without an actual shoreward intrusion, we defined the shoreward transport as the transport that crosses the edge of the stream or the shore-side boundary. We found that the surface shoreward intrusion in the Kuroshio was generally weak and the shoreward intrusion chiefly occurred near the region southwest of Kyushu where 1.8 Sv of the Kuroshio veers shoreward and moves towards Tsushima Strait throughout the year. This well-known intrusion was absent when the shore-side boundary was not used as the interface to define

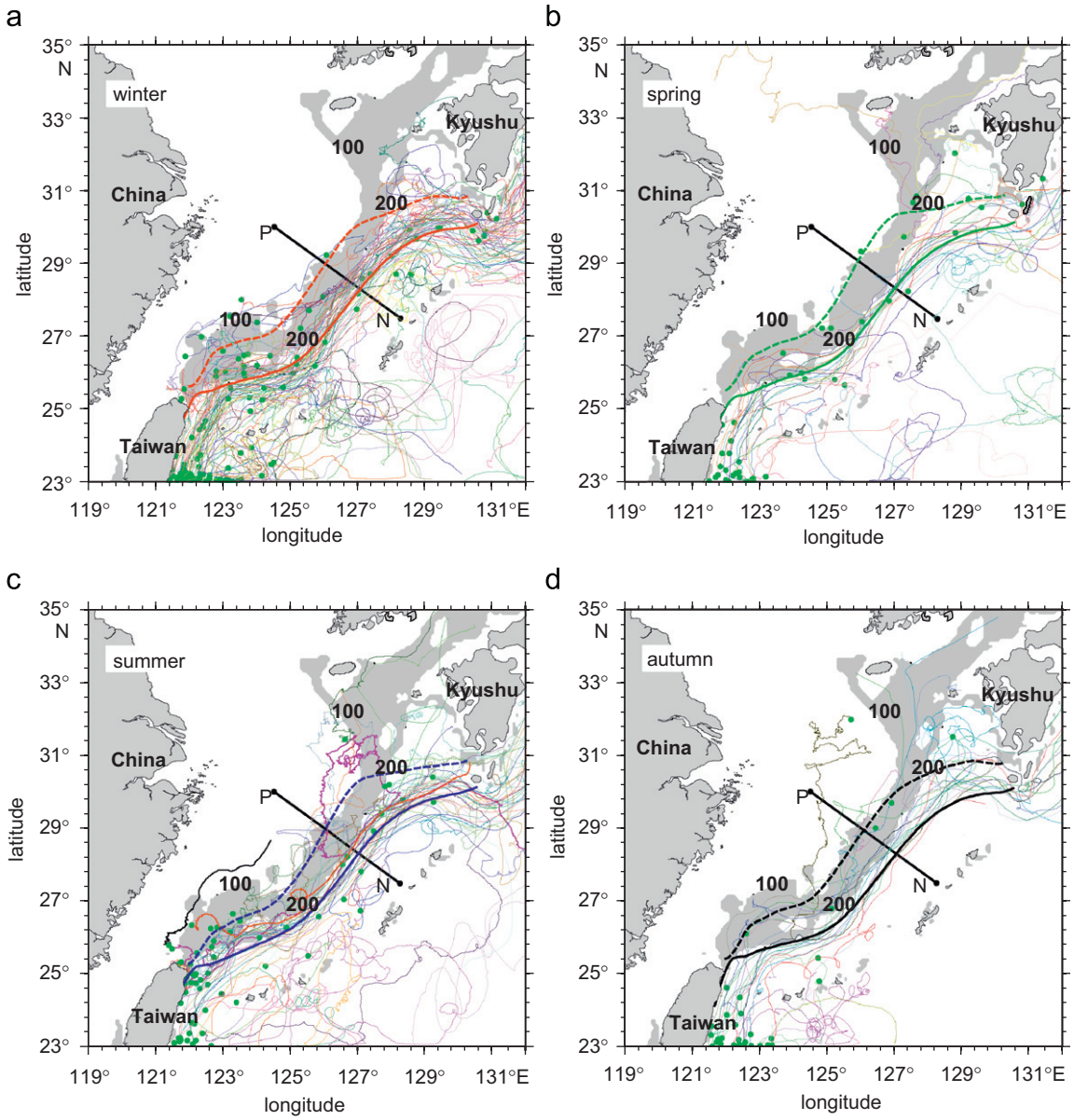

Fig. 14. 19-year (1991–2009) satellite-tracked surface drifter trajectories along the ECS shelf slope for the (a) winter; (b) spring; (c) summer, and (d) autumn. The dashed lines represent locations of the shore-side boundary for each season.

the shoreward transport. The intrusion varied along-stream and there was a strong spatial correlation between the transport of the intrusion and the Kuroshio's intensity on the shore-side of its core. The along-stream shoreward intrusion was mainly governed by the dynamic variation arising from the control of shelf topography on the stream.

The transport in the Ekman layer contributes little to the total along-stream transport in the entire vertical water column, but it plays an important role in the net *surface transport* that crosses the shore-side boundary of the Kuroshio Current. The Ekman current, however, cannot alter the spatial structure of the surface intrusion. The local geostrophic current determines the shoreward intrusion at each isolated portion of the stream. Along the stream, the net surface seaward transport from the geostrophic velocity is due to the offsetting between the shoreward transport north of 127.75°E and the seaward transport south of 127.75°E along the boundary. The net shoreward transport from the bottom Ekman transport and from the transport at depth likely offsets this surface seaward transport, as to be explored.

Acknowledgments

This research was supported by the National Key Basic Research Development Program 2009CB421208. The satellite altimetry data are provided by *Archiving, Validation, and Interpretation of Satellite Oceanographic Data* (AVISO), CNES in France, and the satellite-tracked surface drifter data are from the Integrated Science Data Management/Global Telecommunications System, Fisheries and Oceans Canada (DFO). We thank Xiaopei Lin from Ocean University of China for providing the data used by Ma et al. (2009), and the comments from three anonymous reviewers are appreciated.

References

Andres, M., Park, J.H., Wimbush, M., Zhu, X.H., Chang, K.I., Ichikawa, H., 2008a. Study of the Kuroshio/Ryukyu Current system based on satellite-altimeter and in situ measurements. J. Oceanogr. 64, 937–950.

Andres, M., Wimbush, M., Park, J.H., Chang, K.I., Lim, B.H., Watts, D.R., Ichikawa, H., Teague, W.J., 2008b. Observations of Kuroshio flow variations in the East China Sea. J. Geophys. Res. 113, C05013. doi:10.1029/2007JC004200.

Ducet, N., Le Traon, P.Y., Reverdin, G., 2000. Global high-resolution mapping of ocean circulation from TOPEX/Poseidon and ERS-1 and -2. J. Geophys. Res. 105 (C8), 19477–19498.

Ekman, V.W., 1905. On the influence of the Earth's rotation on ocean currents. Ark. Mat., Astron., Fys. 2, 11.

Gan, J.P., Li, H., Curchitser, E.N., Haidvogel, D.B., 2006. Modeling South China Sea circulation: response to seasonal forcing regimes. J. Geophys. Res. 111, C06034. doi:10.1029/2005JC003298.

Gan, J.P., Cheung, Y.Y., Guo, X.G., Li, L., 2009. Intensified upwelling over a widenedshelf in the northeastern South China Sea. J. Geophys. Res. 114, C09019. doi:10.1029/2007JC004660.

Guo, X.Y., Miyazawa, Y., Yamagata, T., 2006. The Kuroshio onshore intrusion along the shelf break of the East China Sea: the origin of the Tsushima Warm Current. J. Phys. Oceanogr. 36, 2205–2231.

Hsueh, Y., Lie, H.J., Ichikawa, H., 1996. On the branching of the Kuroshio west of Kyushu. J. Geophys. Res. 101, 3851–3857.

Hsueh, Y., 2000. The Kuroshio in the East China Sea. J. Mar. Syst. 24, 131–139.

Hwang, C., 1996. A study of the Kuroshio's seasonal variabilities using an altimetric-gravimetric geoid and TOPEX/POSEIDON altimeter data. J. Geophys. Res. 101 (C3), 6313–6335.

Hwang, C., Kao, R., 2002. TOPEX/POSEIDON-derived space-time variations of the Kuroshio Current: applications of a gravimetric geoid and wavelet analysis. Geophys. J. Int. 151, 835–847.

Ichikawa, H., Beardsley, R.C., 2002. The current system in the Yellow and East China Seas. J. Oceanogr. 58, 77–92.

Isobe, A., 2008. Recent advances in ocean-circulation research on the Yellow Sea and East China Sea shelves. J. Oceanogr. 64, 569–584.

Johns, W.E., Lee, T.N., Zhang, D.X., Zantopp, R., Liu, C.-T., Yang, Y., 2001. The Kuroshio East of Taiwan: moored transport observations from the WOCE PCM-1 array. J. Phys. Oceanogr. 31, 1031–1053.

Lee, J.S., Matsuno, T., 2007. Intrusion of Kuroshio water onto the continental shelf of the East China Sea. J. Oceanogr. 63, 309–325.

Lee, T.N., Johns, W.E., Liu, C.T., Zhang, D., Zantopp, R., Yang, Y., 2001. Mean transport and seasonal cycle of the Kuroshio east of Taiwan with comparison to the Florida Current. J. Geophys. Res. 106, 22143–22158.

Lie, H.J., Cho, C.H., 2002. Recent advances in understanding the circulation and hydrography of the East China Sea. Fish. Oceanogr. 11 (6), 318–328.

Lie, H.J., Cho, C.H., Lee, J.H., Niiler, P., Hu, J.H., 1998. Separation of the Kuroshio water and its penetration onto the continental shelf west of Kyushu. J. Geophys. Res. 103 (C2), 2963–2976.

Le Traon, P.Y., Dibarboure, G., Ducet, N., 2001. Use of high-resolution model to analyze the mapping capabilities of the multi-alitmeter missions. J. Atmos. Oceanic Technol. 18, 1277–1288.

Ma, C., Wu, D., Lin, X., 2009. Variability of surface velocity in the Kuroshio Current and adjacent waters derived from Argos drifter buoys and satellite altimeter data. Chin. J. Oceanol. Limnol. 27 (2), 208–217.

Munk, W.H., 1950. On the wind-driven ocean circulation. J. Meteorol. 7 (2), 79–93.

Nitani, H., 1972. Beginning of the Kuroshio. In: Stommel, H., Yoshida, K. (Eds.), Kuroshio, Phsical Aspects of the Japan Current, University of Washington Press, Seattle, pp. 129–163.

Oka, E., Kawabe, M., 2003. Dynamic structure of the Kuroshio south of Kyushu in relation to the Kuroshio path variations. J. Oceanogr. 59, 595–608.

Pascual, A., Pujol, M.I., Larnicol, G., Le Traon, P.Y., Rio, M.H., Hernandez, F., 2007. Mesoscale mapping capabilities of multisatellite altimeter missions: first results with real data in the Mediterranean Sea. J. Mar. Syst. 65, 190–211.

Qiu, B., Imasato, N., 1990. A numerical study on the formation of the Kuroshio countercurrent and the Kuroshio branch current in the East China Sea. Cont. Shelf Res. 10, 65–184.

Ralph, E.A., Niiler, P.P., 1999. Wind-driven currents in the tropical Pacific. J. Phys. Oceanogr. 29 (9), 2121–2129.

Rio, M.H., Hernandez, F., 2004. A mean dynamic topography computed over the world ocean from altimetry, in situ measurements, and a geoid model. J. Geophys. Res. 99, C12032. doi:10.1029/2003JC002226.

Risien, C.M., Chelton, D.B., 2008. A global climatology of surface wind and wind stress fields from eight years of QuikSCAT scatterometer data. J. Phys. Oceanogr. 38, 2379–2413.

Sun, X.P., Su, Y.F., 1994. On the variation of Kuroshio in East China Sea. In: Zhou, et al. (Eds.), Oceanology of China Seas, vol. 1. , Kluwer Academic, pp. 49–58.

Sverdrup, H.U., Johnson, M.W., Fleming, R.H., 1942. The Oceans, Their Physics, Chemistry and General Biology. Prentice Hall, Englewood Cliffs, NH (p. 719).

Teague, W.J., Jacobs, G.A., Ko, D.S., Tang, T.Y., Chang, K.I., Suk, M.S., 2003. Connectivity of the Taiwan, Cheju, and Korea Straits. Cont. Shelf Res. 13, 63–77.

Zhu, X.H., Ichikawa, H., Ichikawa, K., Takeuchi, K., 2004. Volume transport variability southwest of Okinawa Island estimated form satellite altimeter data. J. Oceanogr. 60, 953–962.